IEICE TRANS. COMMUN., VOL.E86–B, NO.1 JANUARY 2003

PAPER Special Issue on Multiple Access and Signal Transmission Techniques for Future Mobile Communications

Comparative Study of Various Frequency Equalization Techniques for Downlink of a Wireless OFDM-CDMA System

Tomoki SAO[†a)], ***Student Member and*** **Fumiyuki ADACHI**[†], ***Regular Member***

SUMMARY In a wireless OFDM-CDMA system, the data-modulated symbol of each user is spread over multiple subcarriers in the frequency domain using a given spreading code. For the downlink (base-to-mobile) transmissions, a set of orthogonal spreading codes defined in the frequency domain is used so that different users data can be transmitted using the same set of subcarriers. The frequency selectivity of the radio channel produces the orthogonality destruction. There are several frequency equalization combining techniques to restore orthogonality, i.e., orthogonal restoration combining (ORC), control equalization combining (CEC) that is a variant of ORC, threshold detection combining (TDC), and minimum mean square error combining (MMSEC). The ORC can restore orthogonality among users but produces noise enhancement. However, CEC, TDC, and MMSEC can balance the orthogonality restoration and the noise enhancement. In this paper, we investigate, by means of computer simulation, how the BER performances achievable with ORC, CEC, TDC, and MMSEC are impacted by the propagation parameters (path time delay difference and fading maximum Doppler frequency), number of users, pilot power used for channel estimation, and channel estimation scheme. To acquire a good understanding of ORC, CEC, TDC, and MMSEC, how they differ with respect to the combining weights is discussed. Also, the downlink transmission performances of DS-CDMA and OFDM-CDMA are compared when the same transmission bandwidth is used. How much better performance is achieved with OFDM-CDMA than with DS-CDMA using ideal rake combining is discussed.

key words: *OFDM, CDMA, frequency equalization combining, frequency selective channel*

1. Introduction

In mobile radio, the transmitted signal is reflected and diffracted by many obstacles and is received as a multipath signal at a receiver. Hence, the transfer function of a channel varies over a signal bandwidth for wideband signal transmissions. This is called frequency selective fading [1]. For multiple access technique under such a frequency selective channel, a combination of the orthogonal frequency division multiplexing (OFDM) and code division multiple access (CDMA) is considered as a promising technique. In the OFDM-CDMA communication, the data-modulated symbol of each user is spread over multiple subcarriers using a given spreading code defined in the frequency domain [2]–[6]. For the downlink (base-to-mobile) communication, a set of orthogonal spreading codes defined in the frequency domain is used so that different users data can be transmitted using the same set of subcarriers. However, the orthogonality among different users can only be attained if the channel is frequency nonselective. Hence, frequency equalization combining technique is necessary to restore orthogonality.

The orthogonal restoration combining (ORC) [5], [6] perfectly equalizes the frequency selective channel to restore the orthogonality. In ORC, subcarrier components are combined after being weighted in inverse proportion to the channel gain experienced on each subcarrier. Perfect restoration of orthogonality produces the noise enhancement [5]. Therefore, while multi-user interference (MUI) is completely eliminated, the average bit error rate (BER) performance degrades compared to the single user case due to additive white Gaussian noise (AWGN). The noise enhancement in ORC can be suppressed if weak subcarriers are removed from combining. This results in controlled equalization combining (CEC) [6]. Reduction of noise enhancement and orthogonality restoration can be balanced to improve the BER performance. This is achieved by minimum mean square error combining (MMSEC) [7], [8]. In CEC, some of the subcarriers are removed from combining and hence, power loss is produced. MMSEC requires information of the number of users and each subcarrier noise power.

Recently, authors proposed a new frequency equalization combining [9], which is a variant of CEC and is called threshold detection combining (TDC) in this paper. The TDC can more effectively suppress the noise enhancement while minimizing the signal power loss [9]. If the estimate of channel gain falls below a predetermined detection threshold, a large noise enhancement may occur and therefore, unlike CEC, the estimate of channel gain is replaced by the detection threshold. Similarly to CEC, there exists a trade-off relation between reducing the noise enhancement and increasing the MUI due to partial orthogonality destruction. Optimum threshold exists that minimizes the average BER for different channel conditions (i.e., the number

Manuscript received May 17, 2002.
Manuscript revised July 30, 2002.

[†]The authors are with the Electrical and Communication Engineering, Graduate School of Engineering, Tohoku University, Sendai-shi, 980-8579 Japan.
a) E-mail: sao@mobile.ecei.tohoku.ac.jp

of users, the average received signal-to-noise power ratio, the fading maximum Doppler frequency, the pilot power, etc.) [9].

Technical contribution of this paper is as follows. In this paper, we investigate, by means of computer simulation, how the BER performances of OFDM-CDMA downlink achievable with ORC, CEC, TDC, and MMSEC are impacted by the propagation parameters (path time delay difference and fading maximum Doppler frequency), number of users, pilot power used for channel estimation, and channel estimation scheme. To acquire a good understanding of ORC, CEC, TDC, and MMSEC, how they differ with respect to the combining weights is discussed. To the best of authors' knowledge, such a comprehensive performance comparison of the afore mentioned frequency equalization combining techniques has not been reported. Since DS-CDMA is adopted in the 3rd generation mobile communication system [10], it is interesting to compare the downlink transmission performances of DS-CDMA and OFDM-CDMA when the same transmission bandwidth is used. In DS-CDMA, the MUI is produced due to interpath interference in a frequency-selective fading channel and the transmission performance is severely degraded even with ideal rake combining, while in OFDM-CDMA, the MUI can be significantly reduced by the frequency equalization combining as far as the maximum of time delay difference is within the OFDM guard interval. The extent to which the performance is improved with OFDM-CDMA than with DS-CDMA using ideal rake combining is discussed.

The remainder of this paper is organized as follows. Downlink transmission system model of an OFDM-CDMA communication system is presented in Sect. 2. Section 3 overviews ORC, CEC, TDC, and MMSEC. These four equalization combining techniques require channel estimation on each subcarrier. Pilot-aided channel estimation and noise power measurement (for MMSEC only) are presented in Sect. 4. The computer simulation results are presented in Sect. 5 and the BER performances using ORC, CEC, TDC, and MMSEC are compared. Also, comparison is made to DS-CDMA with ideal channel estimation. Section 6 concludes the paper.

2. Downlink Transmission System of a Wireless OFDM-CDMA System

In this paper, OFDM-CDMA downlink is considered. The downlink transmission system is illustrated in Fig. 1. For data modulation, the quadrature phase shift keying (QPSK) modulated data symbol is used. Figure 2 illustrates the slot structure in the time- and frequency-domains. Known OFDM-CDMA pilot symbols are time-multiplexed with data symbol sequence for channel estimation at receivers. The N_p pilot symbols and succeeding N_d data symbol constitutes a slot

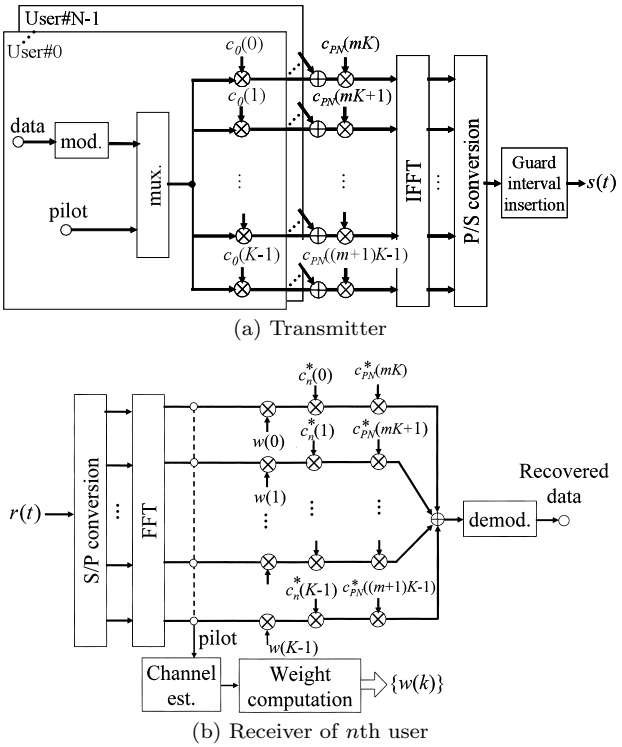

(a) Transmitter

(b) Receiver of nth user

Fig. 1 OFDM-CDMA downlink transmission system.

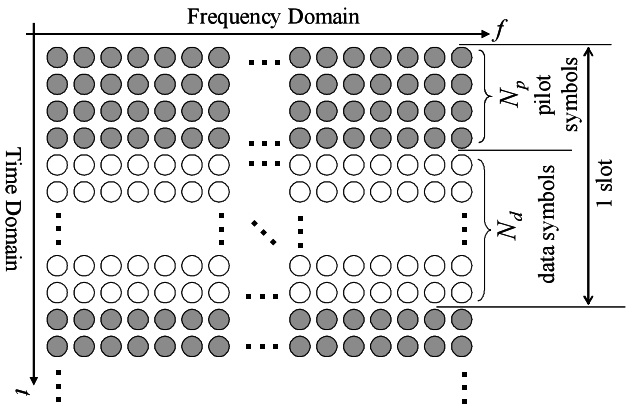

Fig. 2 Slot structure.

of length $N_{slot} = N_p + N_d$ symbols. The pilots are spread over all K subcarriers.

2.1 Transmit Signal Representation

Assume that K orthogonal subcarriers are used. Before modulating the subcarriers, K copies of the mth data modulated symbol of the qth slot for the nth user, denoted by $d_n(qN_{slot} + m)$, is multiplied by the orthogonal spreading sequence $\{c_n(k)\}$ with length K defined in the frequency-domain and then, by the scramble sequence characterized by long pseudo-noise (PN) sequence $\{c_{PN}(i)\}$ with $i = (qN_{slot} + m)K + k$, $k = 0 \sim K - 1$. In Fig. 1, it is assumed that $m = 0$ and $q = 0$ for simplicity. The use of scramble sequence is

to randomize the MUI produced by frequency selective fading. (In the case of cellular system application, the scramble sequences are used in different cell sites as signature sequences in order to separate cell sites [11].) The transmitting OFDM-CDMA signal waveform is obtained by applying the inverse fast Fourier transform (IFFT) [2].

The OFDM-CDMA downlink transmit signal can be expressed in the equivalent baseband representation as

$$\begin{aligned} s(t) = & \sum_{q=-\infty}^{\infty} \sum_{m=0}^{N_{slot}-1} g(t-(qT_{slot}+mT)) \\ & \cdot \left\{ \sqrt{\frac{2S}{K}} \sum_{k=0}^{K-1} u(k, qN_{slot}+m) \right. \\ & \left. \cdot \exp[j2\pi(t-(qT_{slot}+mT))k/T_s] \right\}, \end{aligned} \quad (1)$$

where T_s is called the effective symbol length, S is the average transmit power per user, T is the OFDM symbol length, $T_{slot} = N_{slot}T$ is the slot length, and $u(k, qN_{slot}+m)$ is the mth OFDM-CDMA symbol of the kth subcarrier. The frequency separation between adjacent orthogonal subcarriers is $1/T_s$ (the kth subcarrier frequency is $f_k = k/T_s$). $u(k, qN_{slot}+m)$ can be expressed, using the mth QPSK modulated symbol $d_n(qN_{slot}+m)$ with $|d_n(qN_{slot}+m)| = 1$ for the nth user, as

$$\begin{aligned} & u(k, qN_{slot}+m) \\ & \quad = c_{PN}((qN_{slot}+m)K+k) \\ & \qquad \cdot \sum_{n=0}^{N-1} c_n(k) d_n(qN_{slot}+m) \\ & \qquad \text{for } 0 \le m \le N_{slot}-1 \text{ and } 0 \le k \le K-1, \end{aligned} \quad (2)$$

where N is the number of users in communication. The orthogonal spreading sequences $\{c_n(k)\}$ satisfy

$$\sum_{k=0}^{K-1} c_n(k) c_i^*(k) = \begin{cases} K & \text{for } n = i \\ 0 & \text{for } n \ne i \end{cases} \quad (3)$$

with $|c_n(k)| = 1$, where * denotes the complex conjugate. The guard interval of length T_g is inserted in order to eliminate the inter-carrier interference (ICI) due to frequency selective fading and hence, we have

$$T = T_g + T_s. \quad (4)$$

In Eq. (1), $g(t)$ is the transmit pulse given by

$$g(t) = \begin{cases} 1 & -T_g \le t \le T_s \\ 0 & \text{otherwise} \end{cases}. \quad (5)$$

At the receiver of each user, the received OFDM-CDMA signal waveform is separated into K orthogonal subcarrier components by applying the fast Fourier transform (FFT). Then, the received orthogonal subcarrier components are multiplied by the orthogonal spreading sequence and the scramble sequence both defined in the frequency-domain, and then, summed up to obtain the transmitted QPSK modulated data symbol. When the propagation channel is frequency selective and its frequency transfer function is not constant over the OFDM-CDMA signal bandwidth, the orthogonality among different users may be destroyed. In this paper, various frequency equalization combining techniques are considered and their improvements on the BER performance are compared.

2.2 Frequency Selective Channel

Assuming that the propagation channel consists of L discrete paths having different time delays, its impulse response $h(\tau, t)$ is represented as [12]

$$h(\tau, t) = \sum_{l=0}^{L-1} \xi_l(t) \delta(\tau - \tau_l), \quad (6)$$

where $\xi_l(t)$ and τ_l are the complex channel gain and time delay of the lth propagation path and $\sum_{l=0}^{L-1} E[|\xi_l(t)|^2] = 1$ with $E[.]$ denoting the ensemble average operation. The channel transfer function $H(f, t)$ is the Fourier transform of $h(\tau, t)$ and is given by

$$\begin{aligned} H(f,t) &= \int_0^{\infty} h(\tau, t) \exp(-j2\pi f\tau) d\tau \\ &= \sum_{l=0}^{L-1} \xi_l(t) \exp(-j2\pi f \tau_l). \end{aligned} \quad (7)$$

When $L > 1$, $H(f, t)$ is not anymore constant over the signal bandwidth. Such a channel is called the frequency selective channel. Furthermore, if either transmitter and/or receiver is in movement, the transfer function varies in time and hence, the time selectivity of the channel exists. As a consequence, the wideband mobile propagation channel is doubly selective.

2.3 Received Signal Representation

The receiver structure is illustrated in Fig. 1(b). Applying FFT, the received OFDM-CDMA signal $r(t)$ is resolved into K subcarrier components. First, the received signal is frequency equalized to reduce the frequency distortion produced by frequency selective fading. Transmit data symbol is obtained by multiplying the orthogonal spreading code to K subcarrier components and then, summing up.

The received signal $r(t)$ in the equivalent baseband representation can be expressed as

$$r(t) = \int_{-\infty}^{\infty} h(\tau, t) s(t-\tau) d\tau + n(t), \quad (8)$$

where $n(t)$ is the additive white Gaussian noise (AWGN) having the single sided power spectrum density of N_0. The kth subcarrier component $\tilde{r}(k, qN_{slot}+m)$ is given by

$$\begin{aligned}
&\tilde{r}(k, qN_{slot}+m)\\
&= \frac{1}{T_s}\int_{qT_{slot}+mT}^{qT_{slot}+mT+T_s} r(t)\exp[-j2\pi(t-(qT_{slot}+mT))k/T_s]dt\\
&= \sqrt{\frac{2S}{K}}\sum_{i=0}^{K-1} u(i, qN_{slot}+m)\frac{1}{T_s}\int_0^{T_s}\exp[j2\pi(i-k)t/T_s]\\
&\quad\cdot\left\{\int_{-\infty}^{\infty} h(\tau, t+qT_{slot}+mT)g(t-\tau)\right.\\
&\quad\left.\cdot\exp(-j2\pi i\tau/T_s)d\tau\right\}dt + \tilde{n}(k, qN_{slot}+m), \qquad (9)
\end{aligned}$$

where $\tilde{n}(k, qN_{slot}+m)$ is the noise component due to AWGN characterized by a complex Gaussian process with zero-mean and a variance of $2N_0/T_s$. Assuming that $\max\{\tau_l\}$ is shorter than the guard interval T_g, the integral with respect to τ becomes, from Eq. (5),

$$\begin{aligned}
&\int_{-\infty}^{\infty} h(\tau, t+qT_{slot}+mT)g(t-\tau)\exp(-j2\pi i\tau/T_s)d\tau\\
&= \int_0^{T_s} h(\tau, t+qT_{slot}+mT)\exp(-j2\pi i\tau/T_s)d\tau\\
&= H(i/T_s, t+qT_{slot}+mT). \qquad (10)
\end{aligned}$$

Assuming that $\xi_l(t)$ remains almost constant over the symbol length T,

$$\begin{aligned}
&\xi_l(t+qT_{slot}+mT)\\
&\quad\approx \xi_l(qT_{slot}+mT) \quad \text{for } 0\le t<T \qquad (11)
\end{aligned}$$

and hence, we have

$$\begin{aligned}
&H(i/T_s, t+qT_{slot}+mT)\\
&\quad\approx H(i/T_s, qT_{slot}+mT) \quad \text{for } 0\le t<T. \qquad (12)
\end{aligned}$$

As a result, Eq. (9) can be rewritten as

$$\begin{aligned}
&\tilde{r}(k, qN_{slot}+m)\\
&\approx \frac{1}{T_s}\sqrt{\frac{2S}{K}}\sum_{i=0}^{K-1} u(i, qN_{slot}+m)\\
&\quad\cdot H(i/T_s, qT_{slot}+mT)\\
&\quad\cdot\int_0^{T_s}\exp[j2\pi(i-k)t/T_s]dt + \tilde{n}(k, qN_{slot}+m)\\
&= \sqrt{\frac{2S}{K}}H(k/T_s, qT_{slot}+mT)u(k, qN_{slot}+m)\\
&\quad+\tilde{n}(k, qN_{slot}+m) \qquad (13)
\end{aligned}$$

The nth user's mth symbol $\hat{d}_n(qN_{slot}+m)$ can be obtained by multiplying K subcarrier components by long PN sequence $\{c_{PN}((qN_{slot}+m)K+k);\ k=0\sim K-1\}$ and orthogonal spreading sequence $\{c_n(k)\}$ and summing up. However, as understood from Eq. (13), to reduce the frequency distortion arising from frequency selective fading, the frequency equalization combining is necessary. The combining weight for the kth subcarrier component is denoted by $w(k, qN_{slot}+m)$. After frequency equalization combining, the received data modulated symbol can be written as

$$\begin{aligned}
&\hat{d}_n(qN_{slot}+m)\\
&\quad=\sum_{k=0}^{K-1}\left(\begin{array}{l}\hat{u}(k, qN_{slot}+m)\\ \quad\cdot c_n^*(k)c_{PN}^*((qN_{slot}+m)K+k)\end{array}\right), \qquad (14)
\end{aligned}$$

where $\{\hat{u}(k, qN_{slot}+m);\ k=0,1,\ldots,K-1\}$ is the weighted component of the kth subcarrier and is given by

$$\begin{aligned}
&\hat{u}(k, qN_{slot}+m)\\
&\quad= w(k, qN_{slot}+m)\tilde{r}(k, qN_{slot}+m)\\
&\quad= \sqrt{\frac{2S}{K}}u(k, qN_{slot}+m)\\
&\qquad\cdot\{H(k/T_s, qT_{slot}+mT)w(k, qN_{slot}+m)\}\\
&\qquad+\tilde{n}(k, qN_{slot}+m)w(k, qN_{slot}+m) \qquad (15)
\end{aligned}$$

3. Frequency Equalization Combining

3.1 Orthogonal Restoration Combining (ORC)

The ORC uses the combining weight that is inversely proportional to the channel transfer function $H(k/T_s, qT_{slot}+mT)$ to perfectly restore the orthogonality [3]. However, the channel transfer function is not known to the receiver, channel estimation is required. Channel estimation is described in Sect. 4. Denoting the estimate of the channel transfer function $H(k/T_s, qT_{slot}+mT)$ by $\tilde{H}(k/T_s, qT_{slot}+mT)$, the combining weight $w_{ORC}(k, qN_{slot}+m)$ is given by [5], [6]

$$w_{ORC}(k, qN_{slot}+m) = \frac{1}{\tilde{H}(k/T_s, qT_{slot}+mT)} \qquad (16)$$

and the weighted component $\{\hat{u}(k, qN_{slot}+m);\ k=0,1,\ldots,K-1\}$ of the kth subcarrier becomes

$$\begin{aligned}
&\hat{u}(k, qN_{slot}+m)\\
&\quad= w_{ORC}(k, qN_{slot}+m)\tilde{r}(k, qN_{slot}+m)\\
&\quad= \sqrt{\frac{2S}{K}}\alpha(k, qT_{slot}+mT)u(k, qN_{slot}+m)\\
&\qquad+\frac{\tilde{n}(k, qN_{slot}+m)}{\tilde{H}(k/T_s, qT_{slot}+mT)}. \qquad (17)
\end{aligned}$$

where

$$\alpha(k, qN_{slot}+m) = \frac{H(k/T_s, qT_{slot}+mT)}{\tilde{H}(k/T_s, qT_{slot}+mT)}. \qquad (18)$$

Hence, the mth received symbol $\hat{d}_n(qN_{slot}+m)$ for the nth user is given by

$$\begin{aligned}\hat{d}_n(qN_{slot}+m) &= \sum_{k=0}^{K-1}\hat{u}(k,qN_{slot}+m)c^*_{PN}((qN_{slot}+m)K+k)c^*_n(k)\\ &= \sqrt{\frac{2S}{K}}d_n(qN_{slot}+m)\left(\sum_{k=0}^{K-1}\alpha(k,qT_{slot}+mT)\right)\\ &\quad+\sqrt{\frac{2S}{K}}\sum_{\substack{i=0\\ i\neq n}}^{N-1}d_i(qN_{slot}+m)\\ &\quad\cdot\left(\sum_{k=0}^{K-1}\alpha(k,qT_{slot}+mT)c_i(k)c^*_n(k)\right)\\ &\quad+\sum_{k=0}^{K-1}\frac{\tilde{n}(k,qN_{slot}+m)}{\tilde{H}(k/T_s,qT_{slot}+mT)}c^*_{PN}((qN_{slot}+m)K\\ &\quad+k)c^*_n(k), \end{aligned}\tag{19}$$

where the first term represents the desired signal component, the second term the MUI, and the third term the noise component due to AWGN.

Assuming ideal channel estimation, i.e., $\tilde{H}(k/T_s, qN_{slot}+mT) = H(k/T_s, qN_{slot}+mT)$, $\hat{d}_n(qN_{slot}+m)$ becomes

$$\begin{aligned}\hat{d}_n(qN_{slot}+m) &= \sqrt{2SK}d_n(qN_{slot}+m)\\ &\quad+\sum_{k=0}^{K-1}\frac{\tilde{n}(k,qN_{slot}+m)}{H(k/T_s,qN_{slot}+mT)}\\ &\quad\cdot c^*_n(k)c^*_{PN}((qN_{slot}+m)K+k).\end{aligned}\tag{20}$$

It is understood from Eq. (20) that the ORC can mitigate the MUI completely but enhances the noise components at weak subcarriers. Hence, the BER performance improves but degrades compared to the single user case.

3.2 Controlled Equalization Combining (CEC)

To suppress the noise enhancement produced in the ORC, the CEC removes from combining the subcarrier components of weaker channel gains than the predetermined threshold h_{CEC} [6]. The combining weight $w_{CEC}(k, qN_{slot}+m)$ is given by

$$\begin{aligned}w_{CEC}(k,qN_{slot}+m) &= \begin{cases}\dfrac{1}{\tilde{H}(k/T_s,qT_{slot}+mT)},\\ \quad\text{if } |\tilde{H}(k/T_s,qT_{slot}+mT)|\geq h_{CEC},\\ 0,\quad\text{otherwise.}\end{cases}\end{aligned}\tag{21}$$

As the value of h_{CEC} increases, the noise enhancement reduces but the MUI increases. Hence, there exists an optimum threshold that can balance reduction in the noise enhancement and the increase in the MUI and accordingly minimize the average BER.

3.3 Threshold Detection Combining (TDC)

Unlike the CEC, the TDC uses the weak subcarrier components instead of removing them from combining [9]. The combining weight $w_{TDC}(k, qN_{slot}+m)$ is given by

$$\begin{aligned}w_{TDC}(k,qN_{slot}+m) &= \begin{cases}\dfrac{1}{\tilde{H}(k/T_s,qT_{slot}+mT)},\\ \quad\text{if } |\tilde{H}(k/T_s,qT_{slot}+mT)|\geq h_{th},\\ \dfrac{1}{h_{th}}\dfrac{|\tilde{H}(k/T_s,qT_{slot}+mT)|}{\tilde{H}(k/T_s,qT_{slot}+mT)},\quad\text{otherwise,}\end{cases}\end{aligned}\tag{22}$$

where h_{TDC} is the TDC threshold. Unlike the CEC, since all subcarrier components are used for combining, the TDC has less power loss and the BER performance may be superior to the CEC. Similarly to the CEC, there exists an optimum threshold that can balance the reduction in the noise enhancement and the increase in the MUI. The optimum threshold may be different for CEC and TDC.

3.4 Minimum Mean Square Error Combining (MMSEC)

The MMSEC weighs and combines all the subcarrier components so that the mean square error between the received signal and the desired signal component is minimized [7], [8]. The combining weight $w_{MMSEC}(k, qN_{slot}+m)$, when the number of users in communication is N, is given by

$$\begin{aligned}w_{MMSEC}(k,qN_{slot}+m) &= \frac{\sqrt{2S/K}\cdot\tilde{H}^*(k/T_s,qT_{slot}+mT)}{N|\sqrt{2S/K}\cdot\tilde{H}(k/T_s,qT_{slot}+mT)|^2+2\tilde{\sigma}^2},\end{aligned}\tag{23}$$

where $\tilde{\sigma}^2$ is the estimated noise power per subcarrier, which is assumed to be identical for all subcarriers in this paper. Noise power estimation is described in Sect. 4.2.

4. Pilot-Aided Channel Estimation and MMSEC Noise Power Estimation

4.1 Pilot-Aided Channel Estimation

Figure 3 illustrates the power distribution when two users' data are simultaneously in transmission. On the downlink, the pilots can be shared by all users.

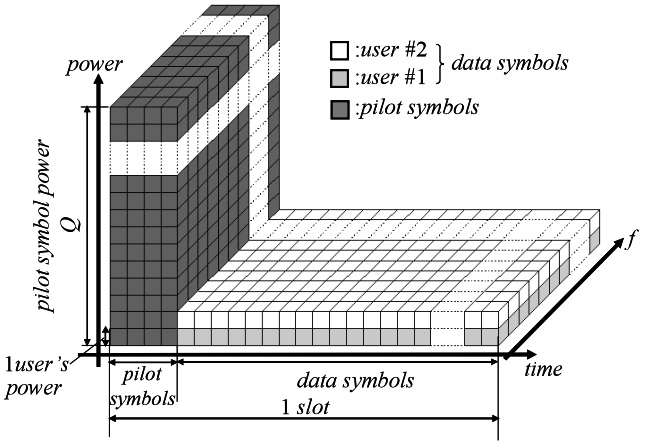

Fig. 3 Power distribution (two-user case).

The received pilot symbol can be represented from Eq. (8) as

$$\begin{aligned}\tilde{r}(k, qT_{slot}+mT) &= \sqrt{2S/K}H(k/T_s, qT_{slot}+mT)u_p(k, qN_{slot}+m) \\ &\quad + \tilde{n}(k, qN_{slot}+m), \quad \text{for } 0 \le m < N_p, \end{aligned} \tag{24}$$

where $\{u_p(k, qN_{slot}+m);\ m = 0 \sim N_p - 1\}$ is the transmitted pilot given by

$$\begin{aligned}u_p(k, qN_{slot}+m) &= \sqrt{Q}\exp(j\pi/4), \quad \text{for } 0 \le m < N_p \end{aligned} \tag{25}$$

with Q representing the pilot-to-data symbol power per user ratio. Assuming that K, Q and $u_p(k, qN_{slot}+m)$ are known to the receiver, channel estimation is carried out by coherently summing up the N_p pilot symbols received at the beginning of each slot. Without loss of generality, we assume to receive the 0th slot. The channel estimate $\tilde{H}(k/T_s, qT_{slot})$ for the kth subcarrier can be expressed as

$$\begin{aligned}\tilde{H}(k/T_s, qT_{slot}) &= \frac{1}{N_p\sqrt{2SQ/K}} \sum_{m=0}^{N_p-1} \tilde{r}(k, qN_{slot}+m) \\ &\quad \cdot u_p^*(k, qN_{slot}+m). \end{aligned} \tag{26}$$

This estimate is used for frequency equalization combining of entire data in a slot. Hence

$$\begin{aligned}\tilde{H}(k/T_s, qT_{slot}+mT) &= \tilde{H}(k/T_s, qT_{slot}) \\ &\quad \text{for } m = N_p \sim N_p + N_d - 1. \end{aligned} \tag{27}$$

4.2 Noise Power Estimation for MMSEC

Estimation of the noise power σ^2 in each subcarrier component is required for MMSEC. This is carried out using pilot symbols [8]. Since K, Q and $u_p(k, qN_{slot}+m)$ are known to the receiver, the unbiased estimation of the noise power $\sigma_k^2 = (1/2)E[|\tilde{n}(k, qN_{slot}+m)|^2]$ of the kth subcarrier can be performed, from Eq. (13), as [15]

$$\begin{aligned}\tilde{\sigma}_k^2 &= \frac{1/2}{N_p - 1} \sum_{m=0}^{N_p-1} \Big| \tilde{r}(k, qN_{slot}+m) \\ &\quad - \sqrt{2S/K}\tilde{H}(k/T_s, qT_{slot}+mT) \\ &\quad \cdot u_p(k, qN_{slot}+m) \Big|^2, \end{aligned} \tag{28}$$

for $N_p > 1$. Assuming that the noise power is identical for all subcarriers, i.e., $\tilde{\sigma}_k^2 = \tilde{\sigma}^2$ for all k, the noise power σ^2 is estimated using

$$\tilde{\sigma}^2 = \frac{1}{K}\sum_{k=0}^{K-1} \tilde{\sigma}_k^2. \tag{29}$$

Table 1 Simulation condition.

Data modulation		QPSK
Spreading codes	Orthogonal code	SF=256
	Scramble code	PN with 4095-chip period
OFDM-CDMA	No. of subcarriers	K=256
	Effective symbol length	T_s=256T_c
	Guard interval	T_g=32T_c (T_g/T_s=1/8)
Rayleigh fading channel	No. of paths	L=2
	Time delay difference	τ=0~5T_c

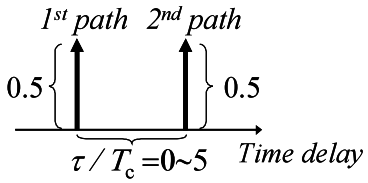

Fig. 4 Power delay profile.

5. Computer Simulation

5.1 Simulation Condition

The simulation condition is presented in Table 1, where T_c denotes the chip rate of DS-CDMA system. The spreading factor (SF) is SF=256 for both OFDM-CDMA and DS-CDMA. The symbol rate of OFDM-CDMA is 8/9 times that of DS-CDMA so that the same bandwidth of $256/T_s$ is used in both OFDM-CDMA and DS-CDMA systems. A two-path Rayleigh fading channel having an equal-power delay profile shape illustrated in Fig. 4 is assumed. It is assumed that $N_p = 4$, $N_d = 60$, and $Q = 256$ unless otherwise stated. Ideal rake receiver is assumed for DS-CDMA [10]. The optimum thresholds of the CEC and TDC are different for

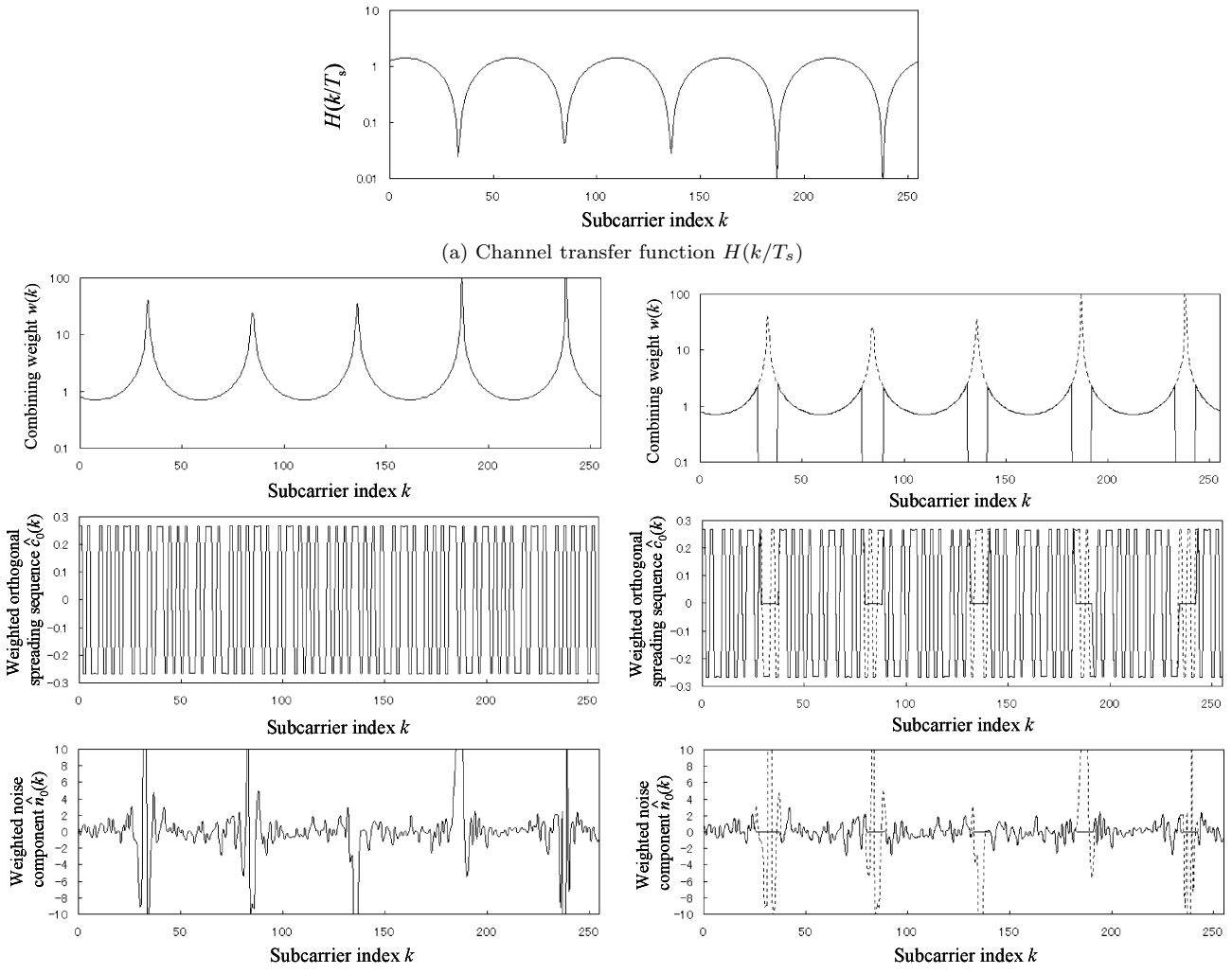

(a) Channel transfer function $H(k/T_s)$

(b) ORC

(c) CEC

Fig. 5 Combining weight $w(k)$, weighted orthogonal spreading sequence $\hat{c}_0(k)$ and weighted noise component $\hat{n}(k)$ when $\tau = 5T_c$.

different channel conditions (i.e., the number of users, the average received signal-to-noise power ratio, the fading maximum Doppler frequency, the pilot power, etc.). Hence, the BER performance curves plotted in subsequent figures are those with the thresholds optimized for each channel condition. Since pilots are used for channel estimation, the use of larger pilot power ratio Q increases the power loss. As mentioned earlier, the pilots can be shared on the downlink by all users. Hence, throughout this paper, the power loss due to pilot insertion is not considered when plotting the BER performance (however, note that the power loss must be take into account when discussing the uplink performance since the dedicated pilots are necessary for each user).

5.2 Ideal Channel Estimation Case

First, we discuss how the combining weight varies in the frequency domain assuming the single user case ($N = 1$). In this case, the weighted component of the kth subcarrier of Eq. (15) reduces to

$$\hat{u}(k) = \left(\sqrt{\frac{2S}{K}} d_0 c_{PN}(k)\right) \hat{c}_0(k) + \hat{n}(k), \tag{30}$$

where $\hat{c}_0(k)$ and $\hat{n}(k)$ are given by

$$\begin{cases} \hat{c}_0(k) = c_0(k)\{w(k)H(k/T_s)\} \\ \hat{n}(k) = w(k)\tilde{n}(k) \end{cases}. \tag{31}$$

For simplicity, the time dependency of the QPSK data symbol, combining weight, the spreading sequence, and the noise component has been dropped. In Fig. 5, the combining weight $w(k)$, the weighted orthogonal spreading sequence $\hat{c}_0(k)$ and the weighted noise component $\hat{n}(k)$ are compared for ORC, CEC, TDC and MMSEC for the given channel transfer function $H(k/T_s)$ when the time delay difference $\tau = 5T_c$. In Figs. 5(c)–(e), the combining weight, the weighted orthogonal spreading sequence and the weighted noise

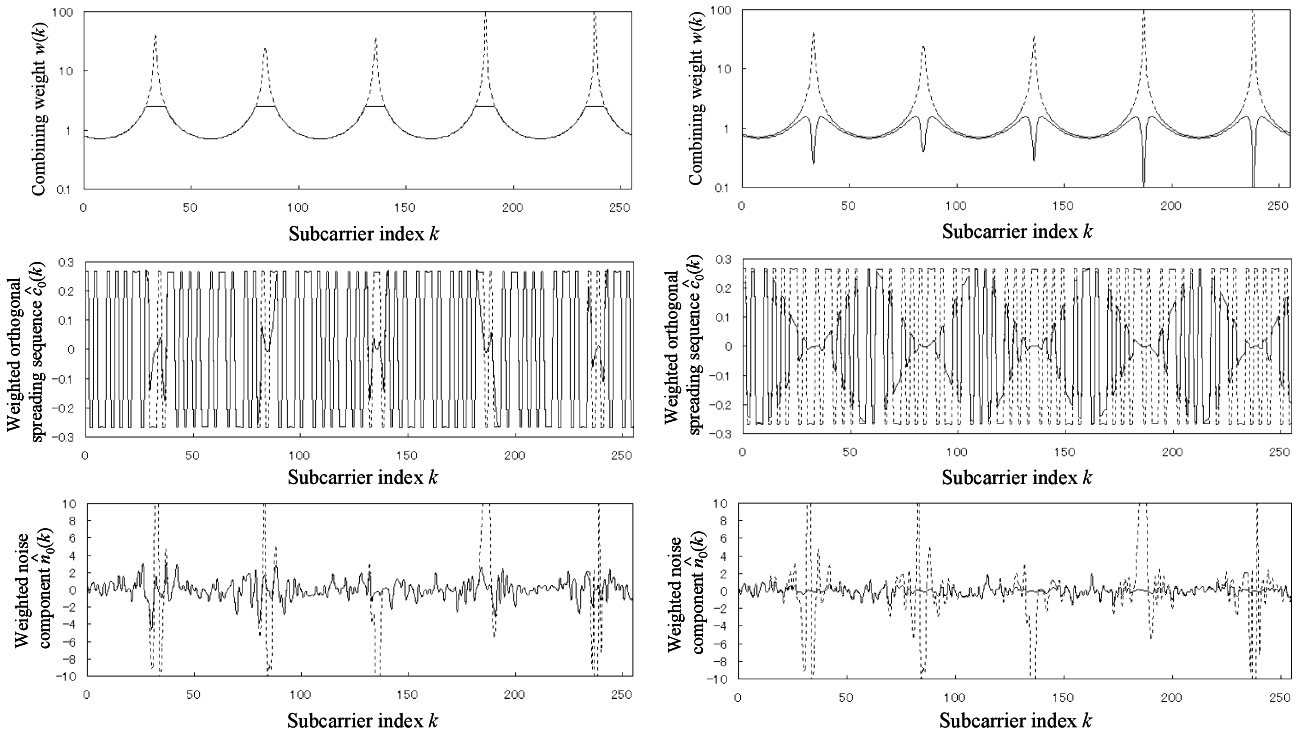

(d) TDC (e) MMSEC

Fig. 5 (Continued)

component for ORC are also plotted by dotted lines for comparison.

The combining weight of ORC is in inverse proportion to the channel gain and thus, a large noise enhancement is observed when the channel transfer function $H(k/T_s)$ drops, while the orthogonal spreading sequence is perfectly restored, i.e., $\hat{c}_0(k) = c_0(k)(c_0(k) = \{11001100\cdots11001100\}$ is assumed.) The CEC sets the threshold and removes the weaker subcarriers than the threshold from combining in order to avoid the noise enhancement, but in turn produces the power loss. On the other hand, the TDC and MMSEC use all the subcarrier components and minimize the power loss while suppressing the noise enhancement.

The BER performances of OFDM-CDMA achievable with ORC, CEC, TDC, and MMSEC are plotted in Fig. 6 as a function of the average received signal energy per information bit-to-AWGN power spectrum density ratio E_b/N_0 for $N = 128$ users and $\tau = 5T_c$. The optimum thresholds are found and used at each E_b/N_0 for CEC and TDC. It is assumed for MMSEC that N is known to the receiver and the noise power estimation is ideal. It can be seen that the ORC offers degraded performance due to the noise enhancement although no error floor is seen. The MMSEC provides the best BER performance, but the BER performance close to MMSEC can be achieved by TDC. However, the BER performance of CEC is about 1.5 dB inferior to that of MMSEC due to the power loss. For

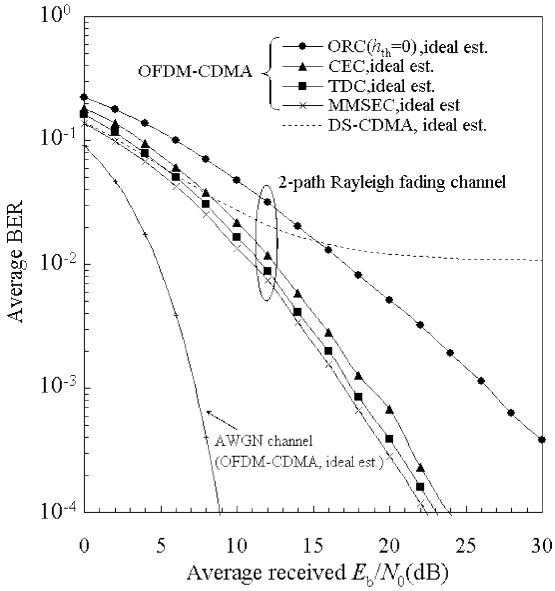

Fig. 6 BER performance comparison for $N = 128$ and $\tau = 5T_c$ with ideal channel estimation.

comparison, the BER performance of DS-CDMA with ideal rake combining is also plotted in Fig. 6. Large error floor due to MUI is seen for DS-CDMA. It is suggested from Fig. 6 that OFDM-CDMA with frequency equalization combining provides a BER performance superior to DS-CDMA in a frequency selective fading channel. However, to obtain a general conclusion,

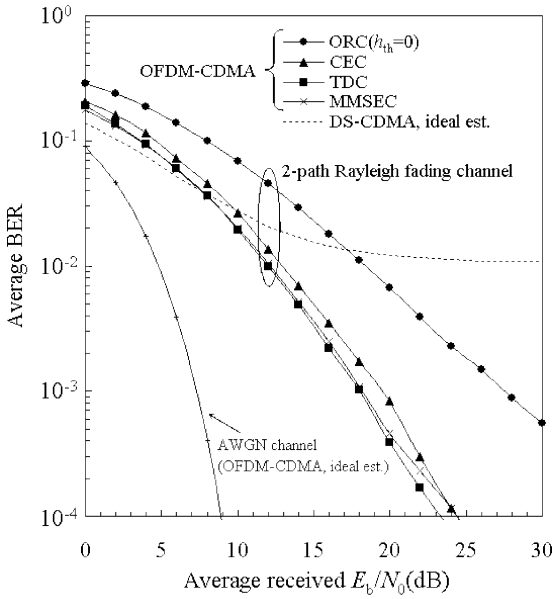

(a) $f_D T_{slot} = 0.0064$

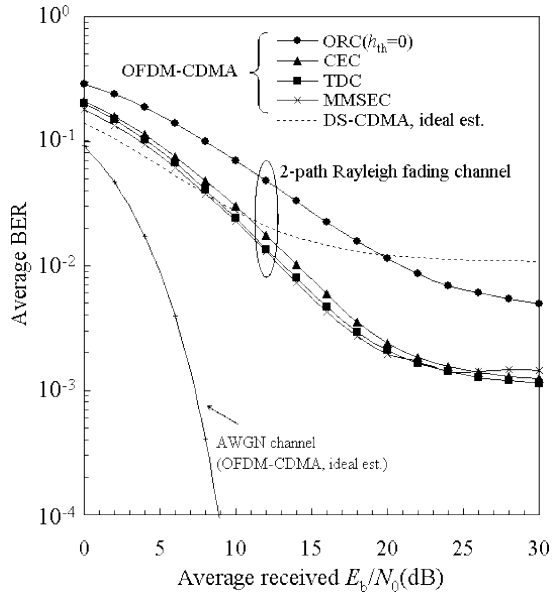

(b) $f_D T_{slot} = 0.032$

Fig. 7 Comparison of BER performances with pilot-aided channel estimation for $N = 128$ users, $Q = 256$, and $\tau = 5T_c$.

more detailed performance comparisons are necessary under various channel conditions (propagation parameters, number of users, etc.).

5.3 Pilot-Aided Channel Estimation Case

Figure 7 compares the BER performances of OFDM-CDMA achievable with ORC, CEC, TDC, and MMSEC using pilot-aided channel estimation for $N = 128$ users, $Q = 256$, and $\tau = 5T_c$. As mentioned earlier, the optimum thresholds for CEC and TDC are used for each channel condition; e.g., they are $h_{CEC} = 0.1$ and $h_{TDC} = 0.2$ at the average $E_b/N_0 = 10$ dB when the fading normalized maximum Doppler frequency $f_D T_{slot} = 0.032$. It can be seen from Fig. 7 that the TDC provides a BER performance close to MMSEC and its required E_b/N_0 for achieving the average BER=0.01 is almost identical when $f_D T_{slot} = 0.032$, while it is slightly larger (about 0.8 dB) than the MMSEC when $f_D T_{slot} = 0.0064$. This is because the channel estimation and the noise power estimation are not perfect and hence, the MMSEC weight computed using Eq. (23) deviates from the optimal one.

For the faster fading case ($f_D T_{slot} = 0.032$), error floor is clearly seen in OFDM-CDMA. This is because the channel estimate obtained using the pilot symbols inserted at the beginning of each slot is used for equalization of all data symbols in a slot while the channel transfer function varies in time over the slot. However, it should be noticed that the error floor values of OFDM-CDMA is much smaller than that of DS-CDMA.

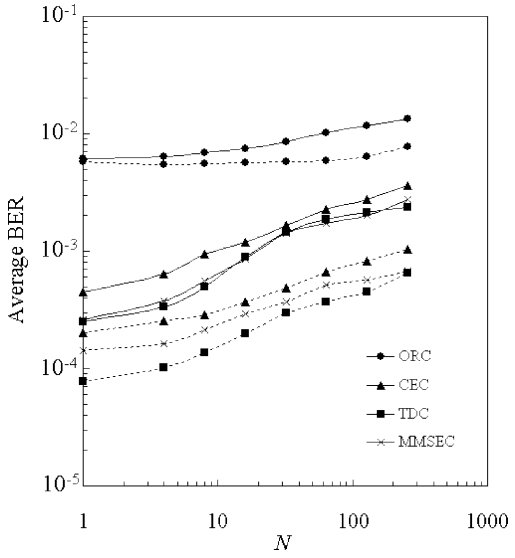

Fig. 8 Effect of number N of users on achievable BER at the average received $E_b/N_0 = 20$ dB for $f_D T_{slot} = 0.0064$ (dotted lines) and 0.032 (solid lines) when $Q = 256$ and $\tau = 5T_c$. $N = 1$–256.

5.4 Impact of Number of Users

How the achievable BER at the average received $E_b/N_0 = 20$ dB (decision errors are mostly produced by channel estimation error) is impacted by the number of users is plotted in Fig. 8 for $f_D T_{slot} = 0.0064$ and 0.032 when $Q = 256$ and $\tau = 5T_c$. It can be seen from Fig. 8 that the BER achieved with ORC is almost insensitive to the number N of users, because almost perfect orthogonality restoration is achieved except for the fast fading case ($f_D T_{slot} = 0.032$). On the other hand, the BERs achieved with TDC and MMSEC are much smaller than those of ORC due to suppression

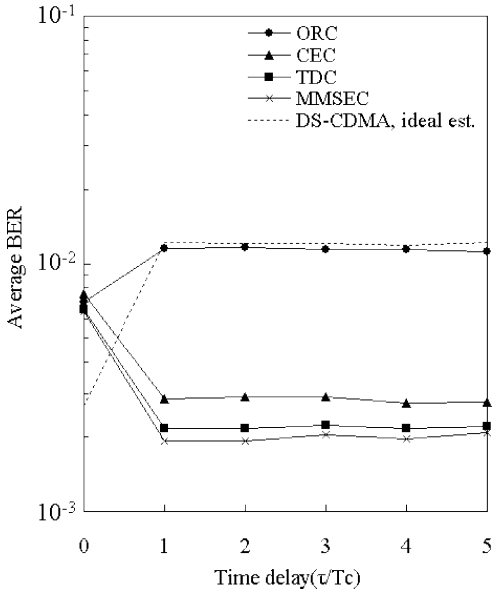

Fig. 9 Effect of time delay difference τ between two paths on achievable BER for $Q = 256$, $N = 128$, the average received $E_b/N_0 = 20\,\text{dB}$, and $f_D T_{slot} = 0.032$.

of noise enhancement; however, the BERs increase as N increases (note that the value of N is known to the MMSEC receiver).

5.5 Impact of Time Delay

When the time delay difference between the two paths is zero (or the propagation channel has a single path), no orthogonality destruction occurs and hence, no MUI is produced. As the time delay difference increases, the channel becomes frequency selective and the orthogonality property among users starts to be destroyed, thereby producing MUI. The use of ORC produces the noise enhancement in exchange for the orthogonality restoration. This results in increased BER as seen in Fig. 9; the same noise enhancement is produced for the time delay difference $\tau \geq 1T_c$. On the other hand, both TDC and MMSEC can reduce the average BERs when $\tau \geq 1T_c$ (or the time delay difference is larger than the FFT sampling period). This is due to the frequency diversity effect, which results from the fact that the contributions of weak subcarrier components to the combined output are made small in MMSEC and are removed in TDC. It can be seen from Fig. 9 that the frequency diversity effect remains constant for $\tau \geq 1T_c$.

5.6 Impact of Pilot Power

So far, we have assumed a large pilot power of $Q = 256$ since it is shared by all users. If the pilot power is reduced, the channel estimation error increases and the noise power estimation for MMSEC may also become inaccurate. How the pilot symbol power impacts the achievable BER performance differently for ORC, CEC, TDC, and MMSEC is interesting to discuss. How the achievable BER is impacted by the pilot power at average received $E_b/N_0 = 10\,\text{dB}$ and $20\,\text{dB}$ is plotted in Fig. 10 for $N = 128$ users and $\tau = 5T_c$. As the pilot power ratio Q reduces from $Q = 256$, the BER gradually increases due to increasing channel estimation error. When decision errors are mostly produced by channel estimation error, i.e., $E_b/N_0 = 20\,\text{dB}$, the BER of MMSEC is found to be much more sensitive to the channel estimation error than CEC and TDC. This is because the MMSEC requires the noise power estimation, which is based on the received pilot symbols. (However, note that the CEC and TDC assume the predetermined optimum thresholds, which must be es-

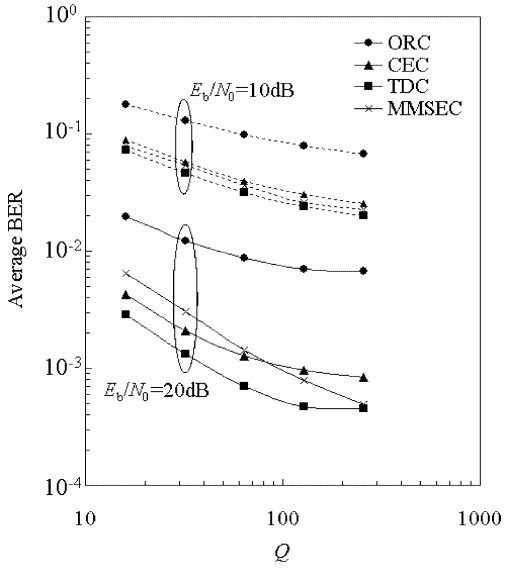

(a) $f_D T_{slot} = 0.0064$

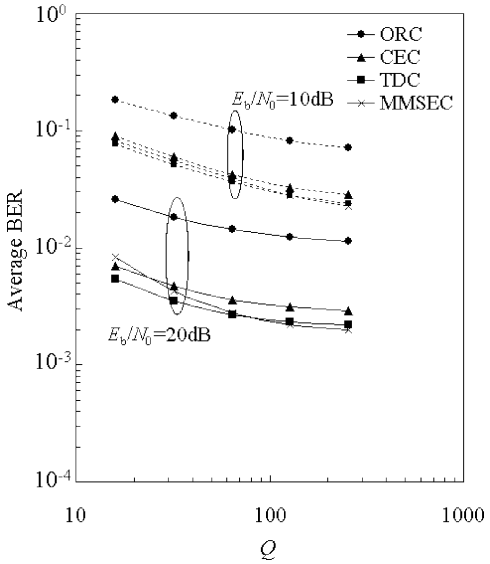

(b) $f_D T_{slot} = 0.032$

Fig. 10 Impact of pilot power on achievable BER for $N = 128$ users and $\tau = 5T_c$.

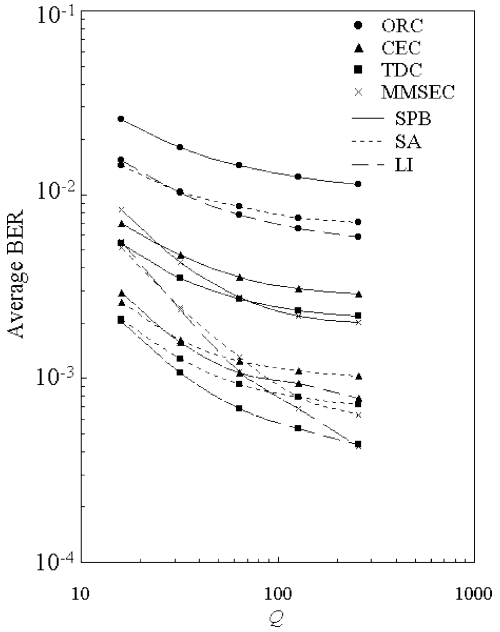

Fig. 11 Impact of channel estimation schemes on achievable BER for $N = 128$ users, the average received $E_b/N_0 = 20\,\mathrm{dB}$, $f_D T_{slot} = 0.032$, and $\tau = 5T_c$.

timated in practical receivers. Adaptive threshold setting is left for a future study.)

5.7 Impact of Channel Estimation Schemes

The results of Fig. 10 imply that the channel estimation scheme may affect significantly the achievable BER performance. So far, to carry out the channel estimation, we used a pilot symbol block time-multiplexed at the beginning of each slot. To improve the channel estimation and/or to reduce the pilot power, pilot symbol blocks of two consecutive slots can be used. The channel estimation schemes using simple average (SA) and linear interpolation (LI) are considered. Eq. (27) becomes

$$\tilde{H}(k/T_s, qT_{slot} + mT) = \begin{cases} \tilde{H}(k/T_s, qT_{slot}), \text{ for SPB} \\ \dfrac{\tilde{H}(k/T_s, qT_{slot}) + \tilde{H}(k/T_s, (q+1)T_{slot})}{2}, \\ \quad \text{for SA} \\ \left(1 - \dfrac{m - (N_p-1)/2}{N_p + N_d}\right) \tilde{H}(k/T_s, qT_{slot}) \\ \quad + \left(\dfrac{m - (N_p-1)/2}{N_p + N_d}\right) \tilde{H}(k/T_s, (q+1)T_{slot}), \\ \quad \text{for LI} \end{cases}, \quad \text{for } m = N_p \sim N_p + N_d - 1 \tag{32}$$

where the channel estimation using the single pilot block (so far we assumed this) is represented by "SPB." How the achievable BER at average received $E_b/N_0 = 20\,\mathrm{dB}$ is impacted by the channel estimation schemes is illustrated as a function of pilot power ratio Q in Fig. 11 for $N = 256$ users, the average received $E_b/N_0 = 20\,\mathrm{dB}$, $f_D T_{slot} = 0.032$, and $\tau = 5T_c$. Using SA and LI can reduce the BER significantly. The reason for this is discussed below. Remember that, for a fast fading channel, the channel transfer function $H(f, t)$ varies over an interval of one slot. The SPB estimates the channel transfer function at the beginning of each slot; hence the channel estimation error becomes larger for the data symbols closer to the end of data slot. This produces error floors. The SA estimates the channel transfer function at the center timing of each slot. This provides the smaller estimation error than the SPB, thereby reducing the error floor. Using LI is more significant, since LI can better track the variations in the channel transfer function. It can be also seen from Fig. 11 that using SA and LI can reduce the pilot power compared to using SPB.

6. Conclusion

In this paper, by means of computer simulation, we investigated how the BER performances of ODFM-CDMA downlink achievable with ORC, CEC, TDC, and MMSEC are impacted by the propagation parameters (path time delay difference and fading maximum Doppler frequency), number of users, pilot power used for channel estimation, and channel estimation scheme. To acquire a good understanding of ORC, CEC, TDC, and MMSEC, how they differ with respect to the combining weights was discussed. Also, in this paper, the downlink transmission performances of DS-CDMA and OFDM-CDMA were compared when the same transmission bandwidth is used. From the computer simulation results, we can draw the following conclusions:

(a) For ideal channel estimation case, TDC yields the BER performance close to MMSEC that provides the best BER performance. The BER performance of CEC is about 1.5 dB inferior to that of MMSEC due to the power loss. No error floors are seen for ORC, CEC, TDC, and MMSEC, while DS-CDMA provides error floor.
(b) When pilot-aided channel estimation is used, the achievable BER performance degrades because the channel estimation is not perfect. However, TDC provides almost the same BER performance as MMSEC. The performance degrades for MMSEC because the MMSEC combining weight computed using Eq. (23) deviates from the optimal one.
(c) The BER performances using TDC and MMSEC are sensitive to the number N of users in communication except for ORC. However, TDC and MMSEC provide much better BER performance than ORC for any number of users.
(d) When the channel is frequency selective (i.e., the

time delay difference is larger than the FFT sampling period), TDC and MMSEC provide better BER performance than ORC. This is due to frequency diversity effect obtained by TDC and MMSEC, but the ORC has the noise enhancement in exchange for the orthogonality restoration.

(e) As the pilot power ratio Q reduces, the BER gradually increases due to increasing channel estimation error. The BER of MMSEC is more sensitive to the channel estimation error than CEC and TDC.

(f) The channel estimation scheme impacts the achievable BER performance in a fast fading channel. The improved channel estimation scheme using SA and LI was considered. The best performance can be achieved with LI, since LI can better track the variations in the channel transfer function. For achieving the same BER, using SA and LI can reduce the pilot power compared to using the single pilot block.

It was suggested that OFDM-CDMA with frequency equalization combining provides a BER performance superior to DS-CDMA in a frequency selective fading channel. However, in this paper, we assumed a simple two-path power delay profile. More detailed performance comparisons are necessary under various channel conditions (propagation parameters, number of users, etc.) to obtain a general conclusion. It has been found that when practical channel estimation is used, error floor is produced in OFDM-CDMA. Application of adaptive channel estimation scheme [13], [14] is effective in a fast fading environment.

References

[1] W.C. Jakes, Jr., ed., Microwave mobile communications, Wiley, New York, 1974.
[2] S. Hara, M. Mouri, M. Okada, and N. Morinaga, "Transmission performance analysis of multicarrier modulation in frequency selective fast Rayleigh fading channel," Wireless Personal Communications, vol.2, pp.335–356, 1996.
[3] L. Hanzo, W. Webb, and T. Keller, Single- and multicarrier quadrature amplitude modulation, John Wiley & Sons, 2000.
[4] M. Helard, R. Le Gouable, J.-F. Helard, and J.-Y. Baudais, "Multicarrier CDMA techniques for future wideband wireless networks," Ann. Telecommun., vol.56, pp.260–274, 2001.
[5] S. Hara and R. Prasad, "Design and performance of multicarrier CDMA system in frequency-selective Rayleigh fading channels," IEEE Trans. Veh. Technol., vol.48, pp.1584–1595, Sept. 1999.
[6] S. Hara and R. Prasad, "Overview of multicarrier CDMA," IEEE Commun. Mag., pp.126–144, Dec. 1997.
[7] A. Chouly, A. Brajal, and S. Jourdan, "Orthgonal multicarrier techniques applied to direct sequence spread spectrum CDMA system," Proc. IEEE GLOBECOM'93, pp.1723–1728, Nov. 1993.
[8] N. Maeda, H. Atarashi, S. Abeta, and M. Sawahashi, "Performance of forward link OFCDM packet wireless access using MMSE combining scheme," Proc. Commun. Conf. IEICE 2001, B-5-48, Sept. 2001.
[9] F. Adachi, M. Sawahashi, and H. Suda, "Wideband DS-CDMA for next generation mobile communications systems," IEEE Commun. Mag., vol.36, pp.56–69, Sept. 1998.
[10] T. Sao and F. Adachi, "Pilot-aided threshold detection combining for OFDM-CDMA down link transmissions in a frequency selective fading channel," IEICE Trans. Commun., vol.E85-B, no.12, pp.2816–2827, Dec. 2002.
[11] H. Atarashi and M. Sawahashi, "Variable spreading factor orthogonal frequency and code division multiplexing (VSF-OFCDM)," 2001 Third International Workshop on Multi-Carrier Spread Spectrum (MC-SS 2001) & Related Topics, pp.113–122, Oberpfafenhofen, Germany, Sept. 2001.
[12] C. Kchao and G.L. Stuber, "Analysis of a direct-sequence spread-spectrum cellular radio system," IEEE Trans. Commun., vol.41, pp.1507–1516, Oct. 1993.
[13] S. Abeta, M. Sawahashi, and F. Adachi, "Adaptive channel estimation for coherent DS-CDMA mobile radio using time-multiplexed pilot and parallel pilot structure," IEICE Trans. Commun., vol.E82-B, no.9, pp.1505–1513, Sept. 1999.
[14] S. Takaoka and F. Adachi, "Pilot-aided adaptive prediction channel estimation in a frequency-nonselective fading channel," IEICE Trans. Commun., vol.E85-B, no.8, pp.1552–1560, Aug. 2002.
[15] A. Papoulis, Probability random variables and stochastic processes, 3rd Edition, p.188, McGraw-Hill, 1991.

Tomoki Sao received his B.S. degree in communications engineering from Tohoku University, Sendai, Japan, in 2001. Currently, he is a graduate student at the Department of Electrical and Communications Engineering, Tohoku University. His research interests include broadband wireless access using OFDM and CDMA for cellular mobile communications systems. He was a recipient of 2002 IEICE Active Research Award in Radio Communication Systems.

Fumiyuki Adachi received his B.S. and Dr.Eng. degrees in electrical engineering from Tohoku University, Sendai, Japan, in 1973 and 1984, respectively. In April 1973, he joined the Electrical Communications Laboratories of Nippon Telegraph & Telephone Corporation (now NTT) and conducted various types of research related to digital cellular mobile communications. From July 1992 to December 1999, he was with NTT Mobile Communications Network, Inc. (now NTT DoCoMo, Inc.), where he led a research group on wideband/broadband CDMA wireless access for IMT-2000 and beyond. Since January 2000, he has been with Tohoku University, Sendai, Japan, where he is a Professor of Electrical and Communication Engineering at Graduate School of Engineering. His research interests are in CDMA and TDMA wireless access techniques, CDMA spreading code design, Rake receiver, transmit/receive antenna diversity, adaptive antenna array, bandwidth-efficient digital modulation, and channel coding, with particular application to broadband wireless communications systems. From October 1984 to September 1985, he was a United Kingdom SERC Visiting Research Fellow in the Department of Electrical Engineering and Electronics at Liverpool University. From April 1997 to March 2000, he was a visiting Professor at Nara Institute of Science and Technology, Japan. He was a co-recipient of the IEICE Transactions best paper of the year award 1996 and again 1998. He is an IEEE Fellow and was a co-recipient of the IEEE Vehicular Technology Transactions best paper of the year award 1980 and again 1990 and also a recipient of Avant Garde award 2000.